Research Article

Study of hydrogen generation and radionuclide release during wet damaged oxide spent fuel storage*

Artem Z. Gayazov[1], Sergey V. Komarov[1], Anton Yu. Leshchenko[1], Ksenia E. Revenko[1], Valery P. Smirnov[1], Elena A. Zvir[2], Pavel A. Ilyin[2], Vladimir G. Teplov[2]

1 *Sosny R&D Company, 4a Dimitrov Ave., Dimitrovgrad, Ulyanovsk reg., 433507 Russia*

2 *JSC «SSC RIAR», 9 Zapadnoye Shosse, Dimitrovgrad, Ulyanovsk reg., 433507 Russia*

Corresponding author: *Artem Z. Gayazov* (gaz@sosny.ru)

Abstract

The paper describes the outcomes of the experiments to study hydrogen and gaseous fission products accumulation during simulations of the wet damaged VVER-440 SNF storage in air-tight canisters with the water drained and no drying conducted. Physical and chemical processes occurring during the damaged oxide SNF storage in wet environment are discussed. The experiments were carried out in two stages: 1) preliminary soaking of fine fuel particles in water in an air-tight canister, 2) water draining and keeping the wet SNF in the air-tight canister.

The experiments were conducted one after another using the same SNF canister and differing only in the SNF soaking temperature, i.e. 25 and 80 °C.

The radionuclide release into the liquid phase during the SNF storage under water was studied. Uranium and cesium isotopic concentrations were found to reach steady values when the SNF is kept under water for more than a month. The kinetics of hydrogen and gaseous fission product accumulation in the gaseous phase during wet storage of the spent fuel in the air-tight canister with the water drained coincide for both experiments. The kinetics demonstrate an abrupt decrease of the hydrogen and gaseous fission product accumulation rate in 46 hours. The data obtained can be applied for development and verification of the damaged SNF behavior models during SNF storage in wet environment under radiolysis.

Keywords

Fire and explosion safety; damaged SNF; VVER-440; radiolysis; hydrogen; gaseous fission products; UO2 dissolution

Introduction

Fire and explosion risk analysis is an important component of the safe handling of spent nuclear fuel and radioactive waste during all phases of the nuclear fuel cycle. Hydrogen is generated during storage of the SNF with leak-tight claddings in humid environment inside an enclosed volume only due to the radiolysis under γ-irradiation, and therefore, the hydrogen accumulation rate can be conservatively evaluated by numerical simulation.

The following additional processes of generation of radiolysis products and oxidative dissolution of the fuel

* Russian text published: Izvestiya vuzov. Yadernaya Energetika (ISSN 0204-3327), 2018, n. 3, pp. 125–136.

which are difficult to be accounted for in the calculations occur when the water contacts leaky spent fuel elements:

– Water radiolysis under irradiation with α- and β-particles with higher linear energy transfer (LET);
– Corrosion of the fuel induced by radiolysis products;
– Other chemical interactions of accumulated radiolysis products with fission products (FP) in the fuel.

Currently, these processes are hard to model, since they occur primarily on the fuel surface and affect each other in a fairly complicated way. Therefore, the only reliable approach to substantiation of fire and explosion safety producing trustworthy results is still physical modeling of the damaged SNF and obtaining experimental dependences of a combustible gas release under anticipated conditions of the SNF storage (handling) with subsequent scaling and extrapolation of the results obtained, if necessary.

The paper describes outcomes of the experiments conducted at the JSC «SSC RIAR» to investigate accumulation of hydrogen and gaseous fission products during simulations of the damaged VVER-440 SNF storage in air-tight canisters with no water inside and no drying performed. Although the obtained results were applied for substantiating fire and explosion safety of the damaged SNF handling under specific storage conditions, they can also be used for development and verification of physical and chemical models characterizing behavior of the damaged SNF during storage in the wet environment with radiolysis occurring.

Behavior of oxide SNF wet environment under radiolysis of water

The basic understanding of physical and chemical processes taking place during storage of uranium dioxide SNF in the wet environment was obtained from the experiments to evaluate the FP and nuclear materials leaching rates in the process of the SNF dissolution (destruction) when the groundwater penetrates the canister in a deep geological repository. A present-day view of the processes is as follows.

The water radiolysis generates primary products both as molecules (H_2O_2, H_2) and radicals ($\cdot HO$, O_2^-, $\cdot HO_2$, e^-_{aq}, $\cdot H$) with the concentrations depending on the type and dose of ionizing radiation (Sattonnay et al. 2001). Interacting with each other the primary radiolysis products can yield secondary products and eventually get recombined. Molecular oxygen is not a primary radiolysis product and comes from secondary chemical reactions and catalytic H_2O_2 decomposition on the fuel surface according to the lumped H_2 reaction:

$$H_2O_2 \rightarrow H_2O + 0{,}5O_2. \tag{1}$$

Although O_2 is involved in oxidation of the nuclear fuel, the primary stable radiolysis product oxidizing the fuel is H_2O_2 (LaVerne and Tandon 2002). Electrochemical investi-

gations demonstrated that H_2O_2 is about 200 times more reactive than O_2 of the same concentration (Shoesmith 2000).

H_2O_2 can either interact with UO_2 through oxidizing U^{IV} into U^{VI} (Barreiro Fidalgo 2017)

$$UO_2 + H_2O_2 \rightarrow UO_2^+ + \cdot HO + HO^-, \tag{2}$$
$$UO_2^+ + HO \rightarrow UO_2^{2+} + HO^- \tag{3}$$

or undergo catalytic decomposition on the UO_2 surface without oxidizing the fuel matrix according to reaction (1) by the mechanism below:

$$H_2O_2 \xrightarrow{UO_2} 2OH \text{ , H2O2} \tag{4}$$
$$H_2O_2 + OH \cdot \xrightarrow{UO_2} H_2O + HO_2 \text{ ,} \tag{5}$$
$$2HO_2 \cdot \xrightarrow{UO_2} H_2O_2 + O_2. \tag{6}$$

The UO_2 dissolution rate in aqueous solutions is dependent on the degree of the fuel surface oxidation conditioned by the redox process. Uranium is considered to dissolve significantly after having reached the $UO_{2.33}$ composition (corresponds to U_3O_7) on the fuel surface (Lucchini et al. 2000).

Two-stage decomposition of radiolytic H_2O_2 and H_2 is suggested in (Wren et al. 2005). The $\cdot HO$ radicals generated at the first phase interact with radiolytic H_2 during the surface-catalyzed decomposition of H_2O_2 causing recombination according to the lumped reaction (9).

$$H_2O_2 + e^- \rightarrow HO + HO^-, \tag{7}$$
$$H_2 + HO \rightarrow \{H_2O + H\} \rightarrow H_2O + H^+ + e^-, \tag{8}$$
$$H_2O_2 + H_2 \rightarrow 2H_2O. \tag{9}$$

However, the uranium oxidative dissolution rate is not conditioned by H_2O_2 concentration. The experiments demonstrated that a uranium release into the solution was much more intensive under irradiation than during leaching tests with H_2O_2 solutions of the same concentration without irradiation. This is due to other radiolysis products participating in the UO_2 oxidation (dissolution) processes under irradiation, for instance, $OH\cdot$ radicals (Eriksen et al. 2012).

The overall process of oxidative dissolution (corrosion) of solid UO_2 includes a sequence of oxidation, dissolution and, under certain conditions, precipitation reactions. The composition of the precipitates will depend on the composition of the solution. Macroscopically, the process can be described by the sequence (Eriksen et al. 2012)

$$UO_2 \rightarrow UO_{2+x} \rightarrow UO_2^{2+} \rightarrow UO_3 \cdot yH_2O, \tag{10}$$

where UO_{2+x} ($U_{1-2x}^{IV} U_{2x}^{V} O_{2+x}$) is a thin intermediate oxidized layer at the UO_2 surface; $UO_3 \cdot yH_2O$ is the U^{VI} precipitates generated during local oversaturation with UO_2^{2+} ions in the thin solution layer at the fuel surface. The precipitates reduce the interaction area, hence suppressing the fuel dissolution. But on the other hand, they restrict mass transport of radiolysis products reducing the H_2O_2 flux from, and scavengers to the SNF surface, and

can lead to the sustainable rate of the SNF dissolution. Uranyl minerals can reduce mobility of key radionuclides and act like the original UO_2 in retaining radionuclides within the fuel matrix. Uranyl minerals can incorporate such radionuclides as Cs and Sr as the major components in their structure (Burns et al. 2012).

Dissolved molecular hydrogen can also be consumed when interacting with the fuel components, thus reducing the uranium concentration in the solution. The so-called hydrogen effect consists in the observed ability of hydrogen to reduce and, in certain cases, completely inhibit the process of the SNF oxidative dissolution. Particles of noble metals Rh, Pd, Ru available in the SNF (so-called ε-particles) catalyze U^{VI} reduction on the fuel surface back to U^{IV} (Barreiro Fidalgo 2017):

$$H_2 + UO_2^{2+} \xrightarrow{\ \varepsilon\ } UO_2 + 2H^+. \qquad (11)$$

Thus, with the fuel destruction still going, after a transient period concentrations of the radiolysis and leaching products (uranium, actinides, FPs) become steady in still water due to the re-precipitation of uranium U^{VI} into the solid phase. These processes govern stationary concentrations of the molecular radiolysis products and, consequently, the rate of the hydrogen and gaseous FP release into the gaseous phase.

In the authors' opinion, the above described behavior of the damaged SNF should be taken into account for the analysis of the experimental results.

Experimental setup and procedure

An in-cell automated experimental setup was developed, manufactured and installed at the Material Test Department of the JSC «SSC RIAR» to investigate behavior of the damaged fuel during simulations of the SNF storage in an air-tight canister.

The experimental setup incorporates an air-tight SNF canister with thermocouples installed on the inner and outer surfaces at different points throughout the height; heating units with an internal water vessel for temperature control outside the canister; pressure monitoring tubing; gas supply and sampling lines; automated control and data acquisition systems. An ASM-142 helium leak detector was used for leak testing to ensure the canister leakage class not lower than 4.

The VVER-440 fuel elements with the following characteristics were selected for the experiments:

– ^{235}U enrichment – 3.6%;
– Average fuel assembly burnup – 27.62 MW·day/kgU;
– Maximum fuel assembly burnup– 32.03 MW·day/kgU;
– Total irradiation time – 649.1 eff. days;
– Cooling period before the experiment – 8 years.

Non-destructive examinations of the fuel elements (visual inspection and imaging, gamma-scanning, diameter measurements in two azimuthal projections, eddy-current testing, measurement of oxide film thickness on the outer cladding surface) demonstrated that conditions of the fuel elements are typical of the VVER-440 fuel after two standard reactor campaigns.

The selected fuel elements were fragmented to remove the fuel pellets that were ground and sieved thereupon. The UO_2 fraction with a particle size of 0.1 - 2.5 mm was weighed and loaded into the canister. Below are the results of two experiments to study behavior of the wet SNF during its storage in the canisters.

Experiment 1 involved 8.75 kg of the prepared UO_2 fraction loaded into the canister and poured with the boric acid dissolved in distilled water ($pH = 4 \pm 0,5$) with a concentration of 24 g/l. In a day, the solution was drained to reduce the impact of radioactive cesium accumulated on the UO_2 surface during its dissolution in water on the concentration measurements of other nuclide; the solution drained was sampled for radiochemical analysis. The canister was refilled with the boric acid solution. The volume of the solution refill was 2422 cm^3. The liquid phase was sampled once a month to determine the nuclide composition of the solution and the quantity of the uranium dissolved. Activity of gamma-emitters in the samples was determined by gamma-spectrometry. Concentrations of Am and Cm were determined by alpha-spectrometry, while those of U and Pu were determined by isotopic dilution mass spectrometry. In three months the boric acid solution was drained from the canister and sampled for radiochemical analysis. Then, the canister was purged with argon thrice, filled up with argon to build up an absolute pressure of 1.5 bar, and tightened. Experiment 1 was carried out for one month with samples of 5 cm^3 each taken. An EMG-20-8 time-of-flight mass spectrometer was used to measure volumetric gas concentrations in the samples.

Upon completion of experiment 1, the canister underwent thermal-vacuum drying, refilled with argon and tightened. After one-month stay the canister was filled up with the boric acid solution with a concentration of 24 g/l to prepare for experiment 2. In a month the boric acid solution was drained from the canister and sampled for radiochemical analysis. Then, the canister was purged with argon thrice, filled up with argon to build up an absolute pressure of 1.5 bar, and tightened, and the heating unit was switched on. Experiment 2 was carried out at a water temperature of 80°C. It was accompanied with gas sampling over the entire period (1 month). Thus, experiment 2 repeated experiment 1 except that it was conducted at a higher temperature.
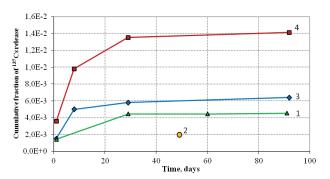
Experiment outcomes and discussion

Tables 1, 2 present data on the SNF soaking in the canister before experiments 1 and 2, as well as radiochemical analysis of the solution samples.

Table 1. Summary of SNF soaking in the solution.

Parameter	Experiment No.1	Experiment No.2
Volume of solution refill, cm^3	2422	2394
Soaking period, days	92	49
Volume of drained solution, cm^3	1931	1901
Volume of solution remaining in canister, cm^3	487	493
Water-UO_2 mass ratio in canister, %	5.6	5.6
Maximum volumetric gamma-activity of drained solution, Bq/ml	$3.3 \cdot 10^7$	$2.0 \cdot 10^7$
Absolute gamma-activity of drained solution, Bq	$6.4 \cdot 10^{10}$	$3.9 \cdot 10^{10}$
Maximum volumetric alpha-activity of drained solution Bq/ml	102	83
Absolute alpha-activity of drained solution, Bq	$2.0 \cdot 10^5$	$1.7 \cdot 10^5$
Quantity of uranium dissolved in boric acid solution during soaking, mg	6.5	8.8±1.6

Figure 1. Kinetics of cesium accumulation in the canisters in experiments no.1 and no.2: 1 – experiment no.1; 2 – experiment no. 2; 3 – experiment D07 (Roth 2015); 4 – experiment L04 (Roth 2015).

Table 2. Activity and nuclide composition of drained solution.

Experiment	No.1					No.2
Sample number	0*	1	2	3	4**	9**
Soaking period, days	1	29	60	91	91	49
Nuclide	Volumetric activity, Bq/ml					
^{137}Cs	$1.3 \cdot 10^7$	$(2.9 \pm 0.3) \cdot 10^7$	$(2.9 \pm 0.3) \cdot 10^7$	$(3.0 \pm 0.3) \cdot 10^7$	$(3.0 \pm 0.3) \cdot 10^7$	$(1.8 \pm 0.2) \cdot 10^7$
^{134}Cs	$1.3 \cdot 10^6$	$(3.1 \pm 0.3) \cdot 10^6$	$(3.2 \pm 0.3) \cdot 10^6$	$(3.0 \pm 0.3) \cdot 10^6$	$(2.9 \pm 0.3) \cdot 10^6$	$(1.5 \pm 0.2) \cdot 10^6$
$\Sigma\gamma$, Bq/ml	$1.4 \cdot 10^7$	$(3.2 \pm 0.3) \cdot 10^7$	$(3.2 \pm 0.3) \cdot 10^7$	$(3.3 \pm 0.3) \cdot 10^7$	$(3.3 \pm 0.3) \cdot 10^7$	$(2.0 \pm 0.3) \cdot 10^7$
Element/nuclide	Concentration, µg/l					
U		2200±110	2300±115	2700±120	1800±100	3500±200
Pu		0.8±0.3	0.9±0.3	1.0±0.3	0.7±0.2	1.3±0.4
^{241}Am		0.02±0.01	0.02±0.01	0.05±0.03	0.02±0.015	0.02±0.01
^{244}Cm		0.002±0.001	0.003±0.002	0.002±0.001	0.004±0.003	0.0043±0.0009
$\Sigma\alpha$, Bq/ml		76±30	102±25	98±20	83±35	83±26

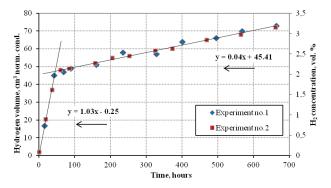* Sample of the solution drained in a day during the first soaking period.
** Sample of the solution drained from the canister after the experiment.

As seen in Table 2, the nuclide compositions quickly reach steady values. It is stated in (Grambow et al. 2000) that, when in contact with irradiated UO_2, simulated or spent fuel under oxidizing conditions, uranium has steady-state concentrations in water of about 10^{-5} M (2400 µg/l) that are close to the theoretical solubility limit for schoepite or other uranyl hydroxide, for instance, becquerelite. As shown in Table 2, the steady-state uranium concentrations in the experiments are close to those values and fall within the range of 1800 – 3500 µg/l.

It also follows from Table 2 that cesium concentration in water remains almost constant. The same is true for the total gamma- and alpha-activity of the solution. Paper (Kolobashkin et al. 1983) describes specific activity of ^{137}Cs and ^{134}Cs in the VVER-440 spent nuclear fuel with similar irradiation parameters and a cooling period of 10 years. For the spent fuel 8 years cooled and used in the experiments, the calculated specific activity makes $2.86 \cdot 10^{12}$ and $3.13 \cdot 10^{11}$ Bq/kgU. The activity ratio is 9.13, which is close to the measured ratio of cesium isotopic activity in the solutions ranging from 9 to 10. However, the calculated cesium volumetric activity in the solutions for the uranium concentrations given in Tables 1 and 2 is lower than the measured one by more than three orders of magnitude (see Table 3).

It is believed that the radionuclide release from the SNF into water is conditioned by two processes, i.e. dissolution of UO_2 grains and an instant release of fission products accumulated either in the fuel-to-cladding gap, or on the grain boundaries. Such a quick release is often called the instant release fraction defined as the relation of the total nuclide quantity in the solution analyzed to the total nuclide quantity in a fuel sample being leached (often using calculated data) (Roth 2015). The calculated cumulative ^{137}Cs release fraction is given in Table 3 and Fig.1. Fig. 1 also shows leaching data for the *BWR* SNF with a burnup of 59 MW·day/kgU and 65 MW·day/kgU in the 10 mM NaCl + 2 mM $NaHCO_3$ solution given in (Roth 2015). The picture demonstrates that the cumulative ^{137}Cs release fraction, although differing in absolute values, behaves similarly in all the experiments, i.e. ^{137}Cs concentrations become steady within a month. Since the instant release fraction is high, changes in cesium concentrations (volumetric activity) due to the UO_2 matrix dissolution induced by radiolysis may remain unnoticed.

When heating the fuel (up to 140 °C), the thermal vacuum drying between experiments 1 and 2 could form new surface, thus providing access to the grain boundaries and resulting in cesium leaching in the next experiment; so, the cumulative ^{137}Cs release fraction in experiment 2 is high enough and makes 45% of the one observed in experiment 1.

Figure 2. Kinetics of hydrogen accumulation in the canisters in experiments no.1 and no.2.

Figure 3. Kinetics of H$_2$, He and Xe accumulation in the canisters in experiment no.1.

Table 3. Calculated and measured average volumetric activity of ^{137}Cs in solutions in SNF soaking experiments.

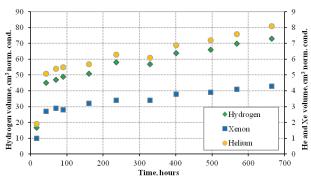| Experiment	Measured uranium concentration, μg/l	Volumetric activity of ^{137}Cs, Bq/ml		Cumulative ^{137}Cs release fraction of
		Calculated uranium concentration	Measurement	
No.1	2200	$6.29 \cdot 10^3$	$2.9 \cdot 10^7$	$1.43 \cdot 10^{-3}$
	2300	$6.57 \cdot 10^3$	$2.9 \cdot 10^7$	$3.18 \cdot 10^{-3}$
	2700	$7.72 \cdot 10^3$	$3.0 \cdot 10^7$	$3.18 \cdot 10^{-3}$
	1800	$5.15 \cdot 10^3$	$3.0 \cdot 10^7$	$3.29 \cdot 10^{-3}$
No.2	3500	$1.00 \cdot 10^4$	$1.8 \cdot 10^7$	$1.98 \cdot 10^{-3}$

Figure 4. Kinetics of H$_2$, He and Xe accumulation in the canisters in experiment no.2.

Fig. 2 shows kinetics of hydrogen accumulation in experiments 1 and 2 (the concentration scale on the right refers to experiment 2 only). The kinetics of hydrogen accumulation in the air-tight canisters in both experiments are identical and can be described by two right lines with the dependencies shown in Fig.2. It proves that hydrogen accumulation does not depend on the ambient temperature, at least within the range of 25–80 °C. The kinetics demonstrates an abrupt decrease in hydrogen accumulation after about 46 hours of the experiment; the hydrogen concentration in the canister, and the volume of hydrogen generated over the first two days is almost the same as that generated over the next month.
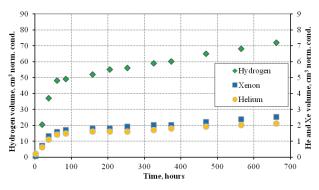
No oxygen was observed in the canister during experiments 1 and 2. All oxygen seemed to be bound to oxidize the uranium dioxide to higher oxides.

Kinetics of helium and xenon accumulation vs. kinetics of hydrogen release are shown in Figures 3, 4. Kinetics of gaseous fission product formation fully correlate with the hydrogen release. According to Henry's law, the partial pressure of the gases in the free volume of the canister is linearly proportional to their concentration in the liquid and the quantity of gaseous fission products is directly proportional to the fuel mass; so, it may be suggested that the degree of the fuel matrix destruction (dissolution) is directly proportional to the concentration of molecular radiolysis products H$_2$O$_2$ and H$_2$ in water.

Apparently, the abrupt decrease in the gas accumulation rate occurred after the uranium solubility limit is reached and U^{VI} precipitated during the SNF destruction

resulting in lower UO$_2$ dissolution rate, greater impact of reverse reactions and suppression of molecular radiolysis products, i.e. hydrogen and hydrogen peroxide. It is noteworthy that ginger-colored precipitates were found at the bottom of the vessel with the solution drained after experiment 2. As stated in (Sattonnay et al. 2001), U^{VI} precipitates on oxidized pellets in the experiments are yellow.

Figures 3, 4 demonstrate that the gaseous fission product yield in the second experiment is far less than in the first one; the He/H$_2$ volumetric ratio decreased fourfold, and Kr/H$_2$ volumetric ratio decreased twofold. Again, this may occur due to the thermal-vacuum drying of the fuel-containing canister between the experiments; the gas partly released from the newly formed UO$_2$ surfaces.

The Xe/Kr volumetric ratio in the canisters in both experiments was 9.5 – 10; this is a typical value for the light-water reactor spent oxide fuel of similar burnup measured during analysis of the gas composition in plenums of the VVER and RBMK fuel rods by laser puncture (Pavlov 2013, Sukhikh et al. 2017).

Conclusions

Experiments were conducted to study hydrogen and gaseous fission products accumulation during simulations of the wet damaged VVER-440 SNF storage in air-tight canisters with the water drained and no drying conducted.

The radionuclide release into the liquid phase during the SNF storage under water was studied, too.

Uranium and cesium isotopic concentrations were found to reach steady values when the SNF is kept under water for more than a month. The cumulative ^{137}Cs release fraction in the water during the SNF leaching made up about $3.3 \cdot 10^{-3}$.

Coincident kinetics of hydrogen and GFP accumulation were obtained for the wet SNF in the air-tight canister at a temperature of 25 and 80 °C with the water drained. Within the first 46 hours of the experiments the hydrogen concentration in the canister quickly reached 2% followed by an abrupt decrease in the hydrogen and GFP accumulation rate. For the next month, about 3% of hydrogen accumulated in the canister.

The data obtained can be applied for development and verification of the damaged SNF behavior models during SNF storage in humid environment under radiolysis.

References

■ Barreiro Fidalgo A (2017) Experimental studies of radiation-induced dissolution of UO_2: The effect of intrinsic solid phase properties and external factors. Doctoral thesis. KTH Royal Institute of Technology: 77. Available at https://www.diva-portal.org/smash/get/diva2:1089678/FULLTEXT01.pdf [Accessed April 6, 2018]

■ Burns PC, Ewing RC, Navrotsky A (2012) Nuclear Fuel in a Reactor Accident. Science, 335: 1184–1188. https://doi.org/10.1126/science.1211285

■ Eriksen TE, Shoesmith DW, Jonsson M (2012) Radiation induced dissolution of UO_2 based nuclear fuel - A critical review of predictive modelling approaches. Journal of Nuclear Materials, 420: 409–423. https://doi.org/10.1016/j.jnucmat.2011.10.027

■ Grambow B, Loida A, Martinex-Esparza A, Diaz-Arocas P, de Pablo J, Paul JL, Glatz JP, Lemmens K, Ollila K, Christensen H (2000) Source term for performance assessment of spent fuel as a waste form. Nuclear Science and Technology Series EUR 19140 EN. IAEA.

■ Kolobashkin VM, Rubtsov PM, Ruzhansky PA, Sidorenko VD (1983) Radiation characteristics of irradiated nuclear fuel. Reference book. Moscow. Atomizdat Publ. [In Russian]

■ LaVerne JA, Tandon L (2002) H_2 production in the radiolysis of water on CeO_2 and ZrO_2. Journal of Physical Chemistry B, 106(2): 380–386. https://doi.org/10.1021/jp013098s

■ Lucchini JF, Sattonnay G, Ardois C, Jegou C, Corbel C (2000) Effects of Water Alpha Radiolysis on the Spent Fuel Matrix, International conference Scientific Research on the Back-end of the Fuel Cycle for the 21st Century. Atalante. Available at http://www.iaea.org/inis/collection/NCLCollectionStore /_Public/32/033/32033983.pdf?r=1 [accessed April 6, 2018]

■ Pavlov SV (2013) Nondestructive ultrasonic methods for testing the research reactor spent fuel. Dimitrovgrad. RIAR Publ., 256 pp. [In Russian]

■ Roth O (2015) A Study of Instant Release Fractions and Matrix Dissolution Rate of Two Fuel Samples Irradiated in Olkiluoto. Working Report 2015–19. Posiva Oy. Studsvik Nuclear AB.

■ Sattonnay G, Ardois C, Corbel C, Lucchini JF, Barthe MF, Garrido F, Gosset D (2001) Alpha-radiolysis effects on UO_2 alteration in water. Journal of Nuclear Materials, 288(1): 11–19. https://doi.org/10.1016/S0022-3115(00)00714-5

■ Shoesmith DW (2000) Fuel corrosion processes under waste disposal conditions. Journal of Nuclear Materials, 282: 1–31. https://doi.org/10.1016/S0022-3115(00)00392-5

■ Sukhikh AV, Sagalov SS, Pavlov SV (2017) Fuel of High Power Channel-type Boiling Water Reactors. Problems&Solutions. Dimitrovgrad. DITI NRNU MEPhI Publ., 184 pp. [In Russian]

■ Wren JC, Shoesmith DW, Sunder S (2005) Corrosion behavior of uranium dioxide in alpha radiolytically decomposed water. Journal of Electrochemical Society, 152: B470–B481. https://doi.org/10.1149/1.2047349